Electric Power Systems Research 234 (2024) 110770

Contents lists available at ScienceDirect

Electric Power Systems Research

journal homepage: www.elsevier.com/locate/epsr

A model-less approach for the optimal coordination of renewable energy sources and DC links in low-voltage distribution networks ☆

Álvaro Rodríguez del Nozal [a], Manuel Barragán-Villarejo [a], Francisco de Paula García-López [a], Goran Dobric [b], Juan Manuel Mauricio [a], José María Maza-Ortega [a,*], Predrag Stefanov [b]

[a] Department of Electrical Engineering, Universidad de Sevilla, Seville, Spain
[b] School of Electrical Engineering, University of Belgrade, Belgrade, Serbia

ARTICLE INFO

Keywords:
Centralized secondary control
DC links
Distribution networks
Online feedback optimization
Renewable energy sources

ABSTRACT

This paper presents a model-less centralized control approach for coordinating Renewable Energy Sources and multiterminal DC links in low-voltage distribution networks. The controller is based on the Online Feedback Optimization technique which is adequate for this part of the power system, characterized by a lack of precise model and real-time information. The paper includes the complete mathematical formulation of the optimization problem and its solution applying the presented strategy. The performance of the proposed centralized controller is evaluated through simulations in the European LV distribution network proposed by the CIGRE Task Force C06.04.02. The results show the benefits that DC links may bring to LV networks due to the release of their radial operation. In particular, the proposed strategy achieves a 7.4 % daily energy loss reduction with respect to the base case. The centralized controller, which operates without a detailed network model and reduced real-time information, enables the use of this technology in LV networks which maximizes the penetration of renewable energy sources.

1. Introduction

Modern power systems become more and more dependent on power electronics to achieve sustainable and environmentally friendly supply of the growing electricity demand. Most of the new technologies driving this paradigm shift, e.g. renewable energy sources (RES) or energy storage systems (ESS), rely on power electronics as an interface with the power grid. This becomes even more relevant in low-voltage (LV) networks, where the active role of citizens in pursuit of a fossil fuel-free future is giving rise to self-consumption, energy communities and microgrids [1,2].

However, a massive RES penetration in LV grids may lead to congestion problems due to their radial operation [3], which can be fixed using traditional network reinforcement techniques [4]. As an alternative, it is possible to take advantage of the advanced control capability that power electronics along with other smart grid technologies may provide [5]. With this regard, the optimal operation of LV grids and microgrids is a subject of growing importance in power systems engineering. Cutting-edge control strategies, energy management and demand-side response techniques have been successfully applied for optimizing the performance and ensuring grid stability in microgrids [6,7] and distribution networks [8,9].

DC links may play an important role in this new situation, providing additional flexibility to accommodate the new active power flows, overcoming all the limitations imposed by the radial network operation, and provide voltage support by independent injections of reactive power. As a matter of fact, DC links have been used in applications for microgrids [10,11] and distribution networks [12,13]. However, the integration of DC links in the distribution network requires a control algorithm able to compute adequate setpoints to fulfill a given operational objective. It is worth noting that this control algorithm has to be adapted to the particular features of the system where the DC link is installed to. As a result, medium-voltage (MV) applications rely on Optimal Power Flow (OPF) techniques since real-time measurements and a detailed network model is available [14–16]. This is not the case, however, for LV grids which lack this information, requiring alternative methods. Previous works have addressed this lack of real-time information resorting to simple control rules based on a reduced set of measurements but, unfortunately, these strategies are not optimal [17]. Recently, a novel control technique, called Online Feedback Optimization (OFO), has been proposed to calculate the optimal setpoints of controllable resources without the need of a detailed

☆ This work has been supported by the European Commission through the project SUNRISE under grant agreement 101079200.
* Corresponding author.
E-mail address: jmmaza@us.es (J.M. Maza-Ortega).

https://doi.org/10.1016/j.epsr.2024.110770
Received 29 September 2023; Received in revised form 20 February 2024; Accepted 17 June 2024
Available online 25 June 2024

network information [18]. The main advantage of OFO is its ability to directly implement the computed variables within the system during each optimization step, thus eliminating the need for an exact network model or the mathematical estimations of system output variables. This technique has been successfully applied in DC microgrids with the objective of maintaining the voltages within the technical limits and sharing the load between the available RES [19,20]. The methodology has been further expanded to encompass AC microgrids, with the aim of optimizing voltage support and the injection of reactive power from a collection of grid-forming RES [21]. Additionally, its applicability has been proven on distribution networks as well [22,23].

This paper proposes to apply OFO as a centralized secondary controller to manage the operation of distributed RES and DC links within a LV distribution network. The objective is to maximize the active power injections from RES, preventing curtailment, while simultaneously minimizing the total power losses and maintaining all the operational magnitudes within the technical limits. To assess the effectiveness of the proposed algorithm, extensive evaluations using the CIGRE LV European benchmark distribution system [24], including a series of unitary and 24-h profile tests, have been conducted. Thus, the main contributions of this paper are:

- The problem definition with a high level of abstraction, allowing the management of any controllable resources regardless of their type.
- An optimal and coordinated management of DC links and RES in LV networks without resorting to a detailed network information.
- The use of an objective function to reduce the RES curtailment while minimizing the total system power losses.

The rest of the paper is organized as follows. Section 2 discusses the problem of interest and establishes the objectives pursued in this work. Section 3 presents the mathematical model and the proposed optimization procedure. Section 4 analyzes the performance of the proposed algorithm through simulation results. Finally, Section 5 points out the main conclusions of the conducted research.

2. Problem description

Consider an AC radial LV network modeled as an undirected graph $\mathcal{G} = (\mathcal{V}, \mathcal{E})$ conformed by a set of buses $\mathcal{V}$ and a set of power lines that interconnect those buses $\mathcal{E} \subseteq \mathcal{V} \times \mathcal{V}$. Customers demanding power from the network are connected in some of the buses, $\mathcal{V}_l \subseteq \mathcal{V}$, while RES injecting power to the grid are within other nodes, $\mathcal{V}_g \subseteq \mathcal{V}$. Note that on a given bus of the AC LV network can be connected a load, a generator or both. In this context, the existence of operational problems in the grid becomes a common event. In fact, if PV generators are considered, overvoltages are likely to occur during the hours of maximum solar irradiation. Conversely, undervoltages may happen during the evening when PV generation decreases and residential loads rise. Since radial networks are considered, the voltage variations at the end of the feeders can compromise the secure operation of the system.

This can be avoided taking advantage of the flexibility provided by the converter-interfaced RES and a centralized control algorithm. It can be considered that RES may arbitrarily set their active power, always below the available primary power, and reactive power injections. At this point, it is considered that the central controller may be able to estimate the available active power at each RES based on real-time meteorological measurements. In addition, a central controller, using adequate real-time system measurements, may compute and dispatch the optimal RES setpoints to achieve a network operation within the technical limits. Nevertheless, in spite of this improvement, the network operation is still radial and overvoltage situations can be solely solved resorting to active power curtailment since reactive power injections are not effective due to the large R/X ratio of LV networks.

With this regard, DC links may provide additional flexibility overcoming the technical barrier imposed by radial network operation [5].

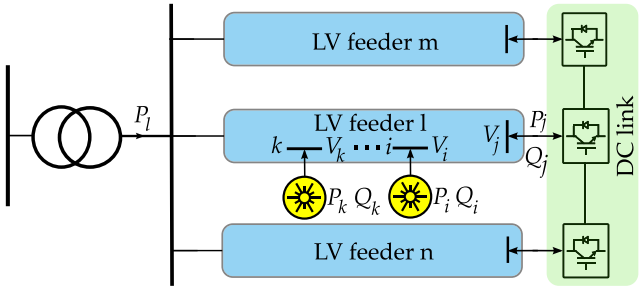

Fig. 1. LV distribution network with details of the nomenclature used in the mathematical formulation.

DC links can be used to control in a flexible manner the active power flow between the interconnected feeders and provide some voltage support by independent reactive power injections. In this manner, DC links are useful to relieve the congestions created by a massive RES integration without resorting to energy curtailment. In case of multiterminal DC links with N terminal VSCs, it is possible to independently control $N-1$ active power and N reactive power injections. Nevertheless, at one of the nodes, the power converter must be in charge of maintaining the DC bus voltage level. Let $\mathcal{V}_{dc} \subseteq \mathcal{V}$ be the set of buses in which there is a connection to the DC-link.

Finally, it should be noted that distribution network models are rarely available in LV grids. Thus, it is proposed to formulate an OFO-based centralized controller to coordinate the operation of the available control assets, i.e. RES and DC links, with the following objectives:

(i) Maximize the RES active power injections to the network minimizing the energy curtailment.
(ii) Guarantee the fulfillment of the network operational constraints.
(iii) Optimize the operation of the DC link and RES to minimize the total power losses in the system.
(iv) Operate the entire network without relying on its detailed model.

3. Mathematical formulation of the problem and adopted solution

This section presents a method for solving the problem previously presented. First, the problem is mathematically formulated. Second, the OFO approach is applied outlining its advantages for a real-time implementation. Finally, a methodology to dynamically adjust a weighting factor included in the objective function is presented.

3.1. Problem formulation

The nomenclature used along the paper is defined with the help of Fig. 1, where some LV feeders coming from a secondary substation with RES and a DC-link terminals are represented. Let $\mathbf{P}$ and $\mathbf{Q}$ be vectors that stack the active and reactive power injections at each bus $k \in (\mathcal{V}_g \cup \mathcal{V}_{dc})$ with controllable resources, i.e. RES or DC links. The components of these vectors are denoted P_k and Q_k respectively. Let $\mathbf{V}$ be a vector that stacks the voltages at these buses, being V_k the nodal voltage at bus k. The active power at the head of the network meshed with the DC link is denoted as P_l. Finally, let $\mathbf{u} = [\mathbf{P}^\top, \mathbf{Q}^\top]^\top$ and $\mathbf{y} = [\mathbf{V}^\top, P_l]^\top$ be, respectively, the inputs and outputs of the centralized controller. Note that the input signals, $\mathbf{u}$, correspond to the optimal setpoints dispatched by the central controller to the controllable resources while the system outputs, $\mathbf{y}$, have to be gathered to this controller.

Using the above notation, the proposed problem can be mathematically formulated as:

$$\mathbf{u} = \arg \min -\beta \sum_{k \in \mathcal{V}_g} P_k + (1-\beta)\hat{P}_{loss}, \quad (1)$$
$$s.t.\ \mathbf{y} = h(\mathbf{u}, \mathbf{w}),$$

$$P_k \le \hat{p} P_{n,k}, \quad \forall k \in \mathcal{V}_g$$
$$P_k^2 + Q_k^2 \le {S_{n,k}}^2, \quad \forall k \in \mathcal{V}_g$$
$$\underline{V} \le V_k \le \overline{V}, \quad \forall k \in (\mathcal{V}_g \cup \mathcal{V}_{dc}),$$

where $\hat{P}_{loss}$ is a variable correlated with the network power losses, h is a function that encapsulates the network power flow equations, being $\mathbf{w}$ a vector that stacks all the unobservable load power injections and β is a weighting parameter. The nodal voltages must be within the limits $\underline{V}$, $\overline{V}$, while the output power of the RES is limited by the rated power of the power converter $S_{n,k}$ and the active power available at the resource. The latter is estimated with respect to the nominal active power of the plant $P_{n,k}$ and is quantified by $\hat{p} \in [0, 1]$, that is a weighting factor estimated from real-time meteorological measurements. The variable $\hat{P}_{loss}$ is defined taking into account the measured active power at the head of the interconnected feeders and the RES active power injections:

$$\hat{P}_{loss} = P_l + \sum_{k \in \mathcal{V}_g} P_k \tag{2}$$

Note that it is not possible to estimate the actual power losses since the active power of the loads are not measured. Regarding the weighting factor, if $\beta = 1$, the total RES active power injection is maximized, thus reducing the power curtailment. Conversely, if $\beta = 0$, the central controller intends to minimize the network power losses. A method to correctly adjust this parameter is presented at the end of the section.

3.2. Proposed method

It is proposed to solve the optimization problem (1) by applying an OFO-based strategy. This consists of applying a classical iterative algorithm for solving optimization problems but dispatching the computed searched variables to the system at each iteration step and, thus, obtaining system outputs instead of estimating them based on imprecise system models. In this work, the augmented Lagrangian of the problem is formulated and solved by applying a primal–dual ascend-descent flow. This methodology has been previously addressed in [19,20], where details of formulation, implementation and performance are comprehensively outlined.

The iterative solution of (1) requires a reformulation in terms of input and output variables as follows:

$$\begin{aligned} \mathbf{u} = \arg \ \min \ & -\beta \mathbf{a}\mathbf{u} + (1-\beta)\mathbf{b}\mathbf{y}, \\ s.t. \ & \mathbf{y} = h(\mathbf{u}, \mathbf{w}), \\ & \mathbf{C}\mathbf{y} \le \mathbf{d}, \mathbf{u} \in \mathcal{U}, \end{aligned} \tag{3}$$

where $\mathbf{C}\mathbf{y} \le \mathbf{d}$ encapsulates the nodal voltage limits, $\mathcal{U}$ defines the feasible area of control inputs $\mathbf{u}$ and vectors $\mathbf{a}$ and $\mathbf{b}$ select the corresponding terms of $\mathbf{u}$ and $\mathbf{y}$ to match the objective functions of (1) and (3).

The augmented Lagrangian is then constructed as:

$$\begin{aligned} \mathcal{L}(\mathbf{u}, \mathbf{y}, \boldsymbol{\mu}, \mathbf{s}) = & -\beta \mathbf{a}\mathbf{u} + (1-\beta)\mathbf{b}\mathbf{y} + \boldsymbol{\mu}^\top (\mathbf{C}\mathbf{y} - \mathbf{d} + \mathbf{s}) \\ & + \frac{\rho}{2} \left\| \mathbf{C}\mathbf{y} - \mathbf{d} + \mathbf{s} \right\|_2^2, \end{aligned}$$

and the iterative algorithm used to solve the problem at the time step m is defined as:

(1) Update slack variables:

$$\mathbf{s}(m+1) = \left[-\frac{1}{\rho} \boldsymbol{\mu}(m) - \mathbf{C}\mathbf{y}(m) + \mathbf{d} \right]_+ .$$

where $[\cdot]_+$ stands for $\max\{0, \cdot\}$.

(2) Update control signals:

$$\mathbf{u}(m+1) = \mathbf{u}(m) - \alpha \frac{\partial \mathcal{L}(\mathbf{u}, \mathbf{y}(m), \boldsymbol{\mu}(m), \mathbf{s}(m+1))}{\partial \mathbf{u}}.$$

(3) Dispatch signals $\mathbf{u}(m+1)$ to the RES and DC link and gather system outputs $\mathbf{y}(m+1)$.

(4) Update Lagrange multipliers:

$$\boldsymbol{\mu}(m+1) = \boldsymbol{\mu}(m) + \rho \left[\mathbf{C}\mathbf{y}(m+1) - \mathbf{d} + \mathbf{s}(m+1) \right].$$

Note that the derivative of the Lagrangian with respect to the system inputs can be obtained as:

$$\begin{aligned} \frac{\partial \mathcal{L}(\mathbf{u}, \mathbf{y}(m), \boldsymbol{\mu}(m), \mathbf{s}(m+1))}{\partial \mathbf{u}} = & -\beta \mathbf{a}^\top + (1-\beta)\mathbf{H}^\top \mathbf{b}^\top \\ & + \mathbf{H}^\top \mathbf{C}^\top \left[\boldsymbol{\mu} + \rho(\mathbf{C}\mathbf{y}(m) - \mathbf{d} + \mathbf{s}(m+1)) \right], \end{aligned}$$

where $\mathbf{H}$ is the sensitivity matrix which measures the variations of the system outputs with respect the inputs. Therefore, it is important to highlight that this OFO-based solving procedure does not need a complete system model to carry out the optimization being possible to guide the system to the optimum simply by using this sensitivity matrix between inputs and outputs. The sensitivity matrix can be obtained by several methods: analytically from the information of an imprecise system model, using a real-time estimation strategy based on filters [25] or applying a *perturb and observe* procedure [19,20], which is the one used in this work.

3.3. Weighting parameter adjustment

It is proposed to dynamically adjust the weighting parameter β according to a prioritization scheme implemented through a two-step procedure. With this regard, it has been considered that the first objective for the network operator is to avoid RES active power curtailment, to maximize the profit of the RES owners, while power loss minimization is a secondary goal. For doing so, the optimization problem (1) is solved with $\beta = 1$. In the OFO framework, the optimization problem is solved by applying the computed inputs in each iteration to the system, which evolves towards the optimal solution and fulfilling the imposed constraints. If there is no need of limiting the RES active power in this optimal scenario, i.e. $P_k = \hat{p} P_{n,k}$, it means that there is room for minimization of power losses. Then, β is automatically changed to 0, i.e. active power losses minimization, the RES active power injections are not considered as OFO variables as long as the active power coming from the primary resource does not change, i.e. $\hat{p}$ keeps constant. This two-step procedure leads to a hierarchy of the control objectives, first maximizing renewable energy penetration and then minimizing system losses.

4. Performance assessment

This section is devoted to evaluating the performance of the proposed OFO-based centralized controller in a LV distribution network with some feeders interconnected by a multiterminal DC link. The selected grid has been proposed by the CIGRE Task Force C06.04.02 for representing European LV networks [24]. This is composed of three main radial feeders as shown in Fig. 2. All the network data including branch parameters and loads are provided in [24]. In addition to the loads connected in different nodes of the network, it is proposed to include PV generation in the buses R01, R04 and R17 of the residential feeder and C11 and C16 of the commercial feeder as in [21]. The 24-h active power profiles of the loads and PV generators are detailed in Fig. 3 using a per unit basis. The corresponding rated power and power factor of the different loads/generators are collected in Table 1. Note that the PV generators operate with unity power factor in the base case. To overcome the radial operation of the system, the three feeders are interconnected by a multiterminal DC link connected at the end of the feeders to the nodes R10, I02 and C09. The VSC in charge of maintaining the DC bus voltage is the one connected to I09, since it is the least loaded feeder and has no PV generation. Although the LV network is characterized by its unbalanced nature, it has been assumed a balanced operation.

To perform the simulations, both the network and the different components connected to it have been modeled in *Python* using the

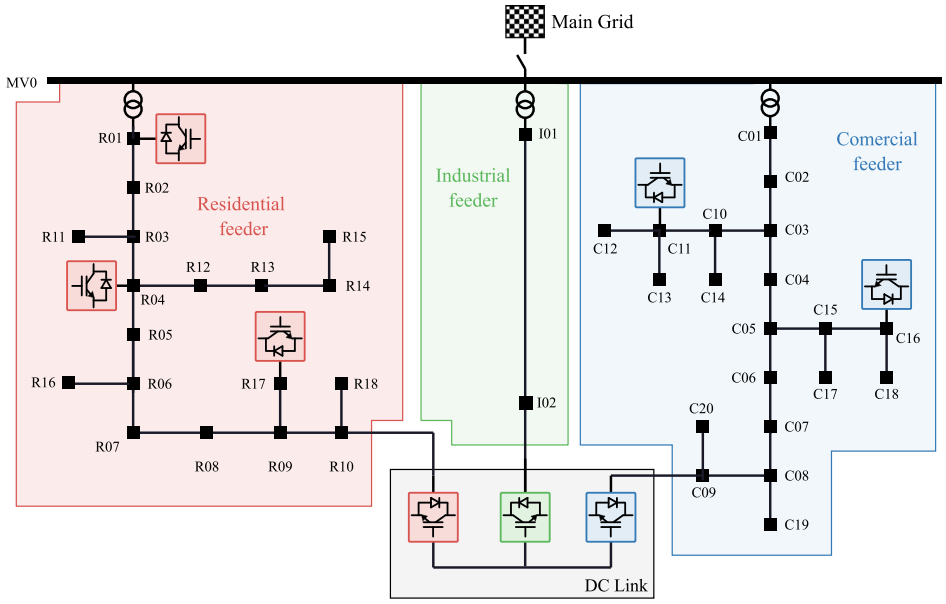

Fig. 2. One-line diagram of the CIGRE European LV benchmark network [24].

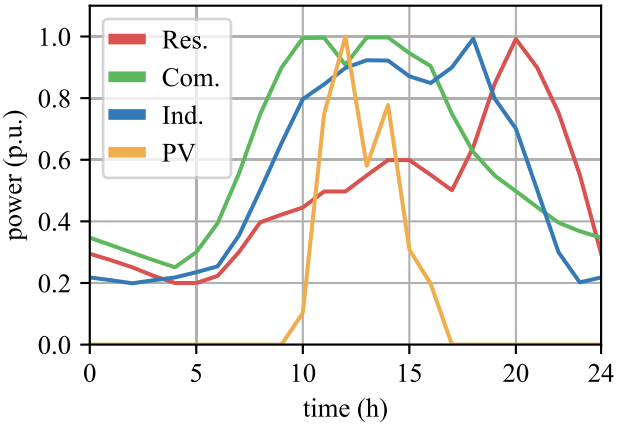

Fig. 3. Load and RES daily power profiles (p.u.).

Table 1
Rated power and power factor of loads and RES.

Node	S (kVA)	$cos\varphi$	Node	S (kVA)	$cos\varphi$
R01	200	0.95	C01	120	0.90
R11	15	0.95	C12	10	0.90
R15	16	0.95	C13	10	0.90
R16	55	0.95	C14	13	0.90
R17	35	0.95	C17	13	0.90
R18	61	0.95	C18	4	0.90
R01	100-PV	1.00	C19	8	0.90
R04	100-PV	1.00	C20	4	0.90
R17	100-PV	1.00	C11	100-PV	1.00
I02	60	0.85	C16	100-PV	1.00

pydae[1] library. The VSC losses have been implemented with the detailed approximations described in [26,27]. Note that the loss model is unknown to the centralized controller, which must adapt to the nonlinearities introduced in the power flows. All simulations have been run on a computer with an i5-10400 CPU at 2.9 GHz with 16 Gb of RAM using 40–70 ms for the execution of each iteration of the algorithm for the unitary tests presented in the next sections.

The next subsections outline a series of unitary and daily profile tests that have been carried out in this benchmark network to evaluate the performance of the controllable assets (DC link and PV generators) operated by the proposed OFO-based centralized controller.

4.1. Unitary tests

The unitary tests are devoted to evaluate the performance of the OFO controller for two different load/generation scenarios: maximum PV generation at 12:00 and maximum demand at 20:00, according to the power profiles shown in Fig. 3. The OFO controller dispatching the multiterminal DC link and RES is compared with (i) a base case, where neither RES control nor DC link is applied, and (ii) an OFO controller managing just the RES and without the DC link. The voltage limits at the network buses are set at ±5% of its nominal value ($400/\sqrt{3}\,V$).

Fig. 4 shows the results for the maximum generation scenario at 12:00. Note that all the subplots are divided into three different sections, divided by gray dotted lines, which correspond to each of the analyzed control scenarios: (i) base case within $t = [0, 10]$ s, OFO controlling RES during $t = [10, 60]$ s and OFO managing RES and DC link within $t = [60, 100]$ s. This time intervals have been chosen to allow the OFO controller to converge to the optimal steady state. The sampling time of the OFO controller has been set to 1 s. The nodal voltages, classified according to their corresponding feeder are shown in the upper subplot, where it is evident an overvoltage situation in the commercial feeder, since no centralized controller is applied and the RES inject the maximum power at unity power factor as shown in the middle subplots of Fig. 4. This situation is improved when the centralized OFO controller dispatches the RES, $t = [10, 60]$ s, reducing their active power injections and absorbing reactive power. This control action reduces the nodal voltages in the commercial feeder with respect to previously analyzed base case. Note that the nodal voltages in the residential and industrial feeders remain constant, since the OFO controller does not change the PV setpoints due to the absence of voltage violations. This control action helps to operate the system within the technical limits, but at the cost of active power curtailment. The incorporation of the DC link as a control asset, $t = [60, 100]$ s, eliminates the technical barrier imposed by the radial network operation. The first noteworthy action is that the PV generators return to their original state, i.e. maximum operating point and null reactive power. This is

[1] https://pydae.readthedocs.io/

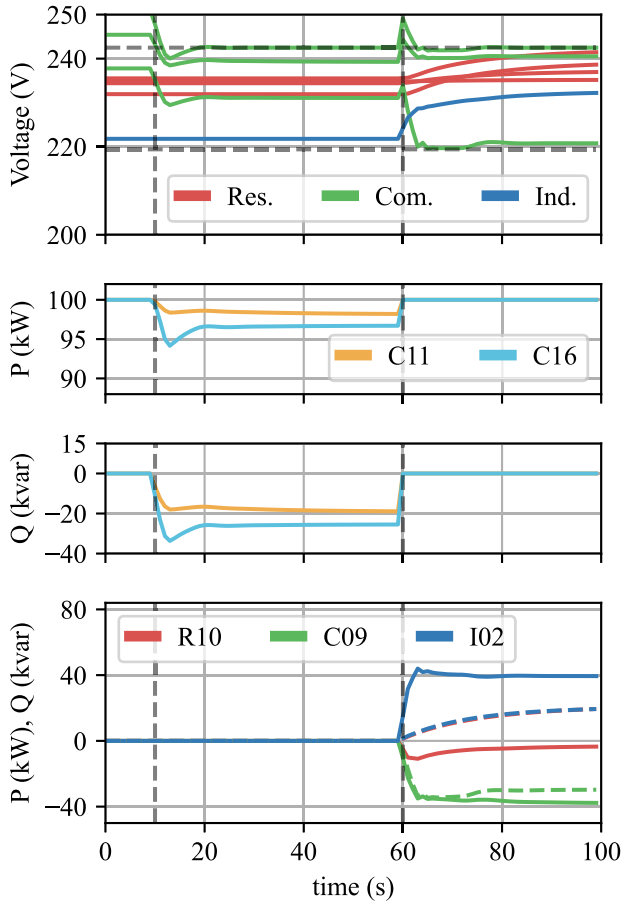

Fig. 4. Unitary testing with maximum RES generation (12:00). (i) Nodal voltages, (ii) RES active power injections in commercial feeder (iii) RES reactive power injections in commercial feeder (iv) DC-link active (solid line) and reactive power injections (dashed line).

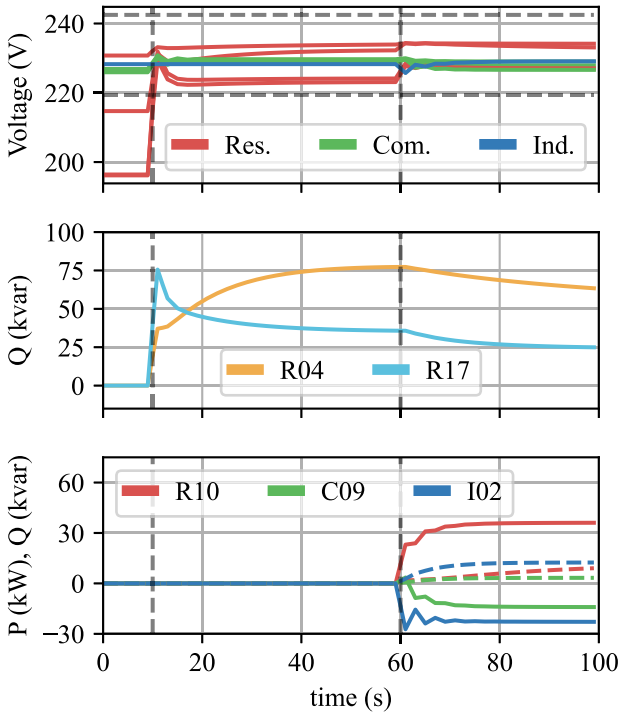

Fig. 5. Unitary testing with maximum load (20:00). (i) Nodal voltages, (ii) RES reactive power injections in commercial feeder (iii) DC-link active (solid line) and reactive power (dashed line) injections.

possible thanks to the DC link starts to exchange active power between the interconnected feeders. This implies that the OFO controller can work with the objective of minimal losses. As can be seen in the lower subplot of Fig. 4, the DC-link active power (solid line) is negative in the residential and commercial feeders, where the RES are connected to. This means that part of the RES active power generated in these feeders is transferred to the industrial one. Note that the active power from the commercial feeder is large to avoid overvoltage violations. In addition, the DC-link VSCs inject/absorb reactive power (dashed line) to control the voltages which are affected by the imposed active power transfer. Thus, the DC-link VSC connected to the commercial feeder absorbs reactive power to reduce the voltages of its buses and favor active power transfer. Conversely, the DC-link VSC within the industrial feeder injects reactive power to increase the voltages and reduce the system power losses. Note that the DC link completely modifies the power flows in the LV network and, therefore, the nodal voltages change totally with respect to the previous radial operation. In fact, it is worth noting that the industrial feeder voltages increase since the load is partly fed by the DC-link. In any case, the nodal voltages remain within the technical limits.

Fig. 5 presents the results for the maximum demand at 20:00 following the same approach than in the previous case. Note that the RES active power injections are null in the analyzed hour. The analysis of the nodal voltages at the top plot of Fig. 5 evidences severe under-voltage problems in the residential feeder, due to its large demand, in the base case. This situation can be solved by the centralized OFO controller dispatching the RES, $t = [10, 60]$ s. In fact, note that all the nodal voltages within the residential feeder are within the imposed technical limits. For doing so, the RES connected to the buses R04 and R17 inject significant reactive power, particularly in the bus R04 reaching up to 75% of the rated power. When the multiterminal DC link is added as control action, the nodal voltages within the residential feeder raise because part of the load is fed from the end of the feeder. It is worth noting that the DC-link power flows change completely with the previous analyzed case. In this scenario, the residential feeder load is supplied through the industrial and commercial feeders as shown in the bottom subplot of Fig. 5. The DC-link terminals also inject some reactive power (dashed line) to maintain the voltage within the limits since it is a highly loaded scenario without generation. Finally, the improvement in the nodal voltages of the residential feeder reduces the need of RES reactive power injections as shown in the middle plot of Fig. 5.

It is important to note that, although the presented algorithm operates without relying on a network model, the results obtained in steady state are identical to those of a conventional model-based OPF [21].

4.2. 24 h profile

This subsection presents the results of 24-h simulation analyzing the global impact of the proposed controller. The simulation has been performed using the daily load curves presented in Fig. 3 with updates every hour. The results are compared with the base case and an OFO controller dispatching the RES, in a similar manner than in the previous subsection. In this case, box plots are used to analyze in an aggregated form the results. These plots represent the first to third quartile of the data, with a line at the median. The whiskers extend from the box to the maximum and minimum values. The analyzed variables are the nodal voltages, and the RES and multiterminal DC-link active and reactive power injections.

Fig. 6 shows the box plots of the voltages of those nodes where the RES and the DC link are connected to within the residential (R01, R04, R10 and R17), industrial (I02) and commercial (C09, C11 and

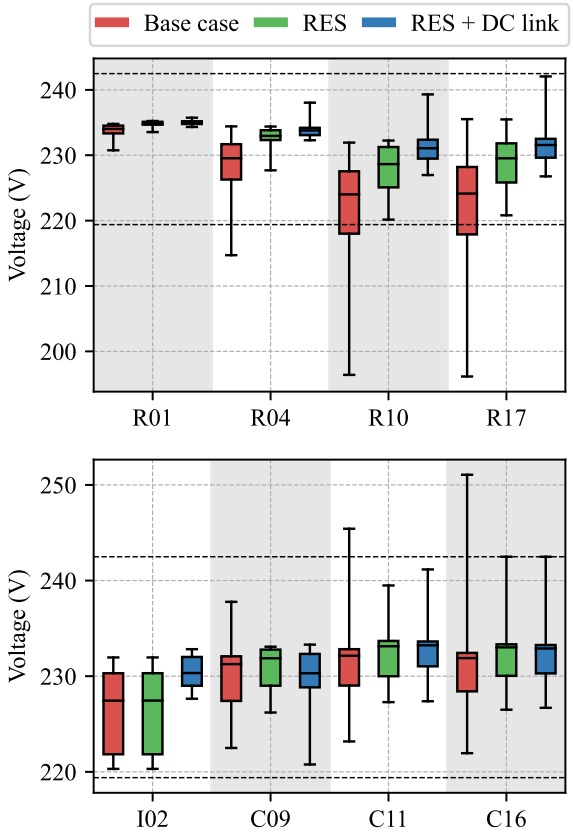

Fig. 6. 24-h profile test. Box plots of the RES and DC-link nodal voltages.

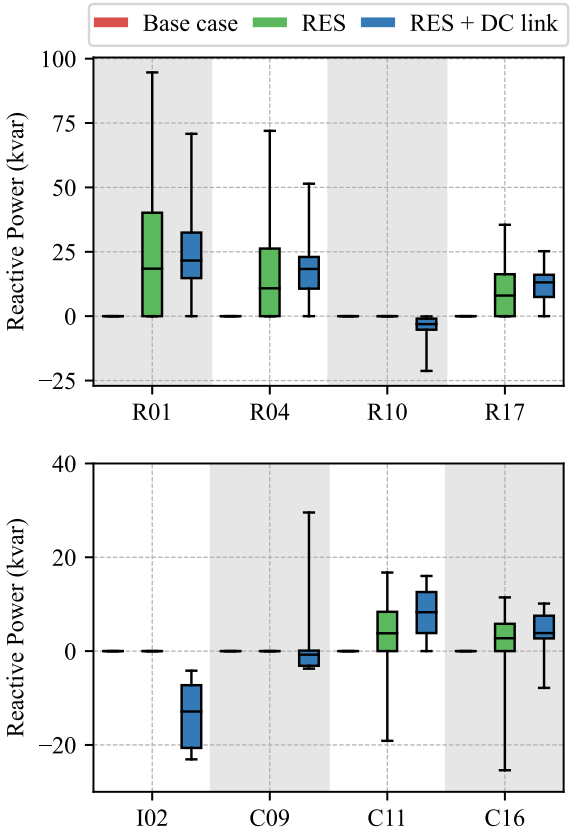

Fig. 7. 24-h profile test. Box plots of the RES and DC-link reactive power.

C16) feeders. The analysis of the voltages in the residential feeder shows some undervoltage problems in the base case, where no control is applied, in addition to large voltage variations along the day. The commercial feeder also presents some voltage problems but in an opposite manner due to the large RES penetration.

Note that these voltage problems are solved with the application of the OFO-based controller dispatching the RES, since all the box plots remain within the permissible voltage band. This is achieved resorting to active power curtailment, about a 0.4% in the analyzed case, and reactive power injections, which are depicted in Fig. 7. It is worth noting that these reactive power injections are consistent with the voltages presented in Fig. 6. Thus, RES connected to the residential feeder inject reactive power to raise the voltage. Moreover, note that OFO-based controller distributes unequally the reactive power among the existing RES due to the different X/R ratio of the network impedance at their corresponding connection node. The effect of the reactive power injection on node R01, close to the distribution transformer with a higher X/R ratio, is much more effective than in other downstream nodes, e.g. R04. Regarding the results within the commercial feeder, the box plots of reactive power injections extend for positive and negative values, i.e. capacitive or inductive, which is consistent with the change of the voltages with respect to the base case depicted in Fig. 6. On the one hand, the median voltage increases due to the reactive power injections but, on the other hand, those whiskers above the maximum voltage in the base case are within the limits thanks to the reactive power consumption.

These results are improved in case of adding the DC link as a new control asset. Fig. 6 reveals that not only the nodal voltages increase but also their variations along the day are reduced. Note that this voltage increase is due to the controllable loop created by the DC link, which clearly overcomes the limit imposed by the radial network operation. As a matter of fact, the active power flows imposed by the DC link depend on the generation/load scenario as shown in Fig. 8. Thus, the DC-link active power injections in the residential and industrial feeders, R10 and I02 respectively, are either positive or negative which is consistent with the results obtained in the unitary tests and depicted in Figs. 4 and 5. Moreover, the new flexibility provided by the DC link releases the RES reactive power requirements as shown in Fig. 7, particularly to the RES connected to R01 and R04.

Finally, and regarding the total power losses of the system used as objective function of the OFO-based controller, it should be emphasized that the DC link achieves a 7.4% of daily energy loss reduction with respect to the base case (449 kWh). This is energy saving is significant considering that it represents an additional 4.5% with respect to the case where the control assets are reduced just to RES.

5. Conclusions

This paper has presented a model-less approach to perform an active operation of a LV distribution network taking advantage of distributed RES and a multiterminal DC link as control assets. For this purpose, a centralized OFO-based controller is developed with the aim of dispatching these controllable devices without resorting to a detailed network model. In fact, this approach is a reasonable strategy for LV networks since the lack of information prevent the use of classical OPF techniques, widely applied in transmission and MV distribution applications where network models and massive real-time measurements are available. The model-less controller seeks to maintain the operational network constraints with minimum power losses and without resorting to RES active power curtailment. For this purpose, a complete mathematical formulation including how to implement the OFO controller has been described. The performance assessment of the proposed controller has been tested by different simulation scenarios using the European LV distribution network proposed by the CIGRE

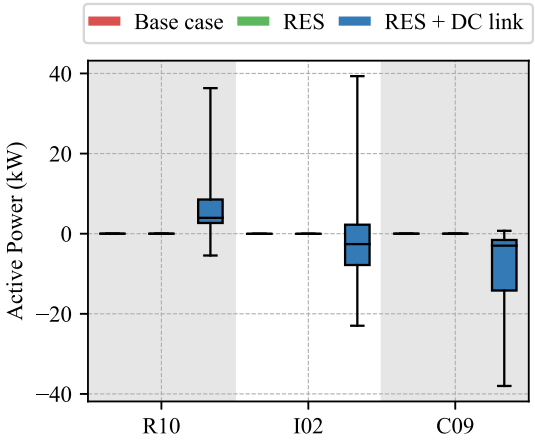

Fig. 8. 24-h profile test. Box plots of the DC-link active power.

Task Force C06.04.02. Two unitary tests have been carried out to analyze the performance on totally opposite generation/load scenarios. The results have revealed that the OFO controller dispatching the DC link and the RES is able to improve the network operation adapting the network power flows to each required situation with a good convergence characteristic. In addition, a 24-h daily test simulation has been performed with the objective of analyzing the overall impact on the system. The results have evidenced that the OFO controller dispatching the DC link may bring several benefits to the active operation of LV distribution networks in terms of voltage profiles, reduced RES reactive power requirements and system power losses. Specifically, daily energy losses are reduced by 7.4% compared to the base case and by an additional 4.5% compared to the case where the control assets are reduced to RES. As a result, the multiterminal DC-link technology along with the proposed model-less control approach unlock the required flexibility to operate actual LV distribution networks with a massive RES penetration.

The future research will address the unbalanced nature of LV distribution networks, incorporating novel control objectives for reducing the imbalance and taken advantage of new control assets like transformers equipped with On Load Tap Changers and electrical vehicle chargers.

CRediT authorship contribution statement

Álvaro Rodríguez del Nozal: Conceptualization, Formal analysis, Methodology, Software, Writing – review & editing. **Manuel Barragán-Villarejo:** Conceptualization, Formal analysis, Methodology, Writing – review & editing. **Francisco de Paula García-López:** Conceptualization, Validation, Writing – review & editing. **Goran Dobric:** Conceptualization, Formal analysis, Methodology, Writing – review & editing. **Juan Manuel Mauricio:** Conceptualization, Formal analysis, Methodology. **José María Maza-Ortega:** Conceptualization, Formal analysis, Funding acquisition, Supervision, Writing – review & editing. **Predrag Stefanov:** Conceptualization, Funding acquisition, Writing – review & editing.

Declaration of competing interest

The authors declare that they have no known competing financial interests or personal relationships that could have appeared to influence the work reported in this paper.

Data availability

All the data used in this work has been included in the manuscript.

References

[1] Australian Energy Council, Solar Report, Australian Energy Council, 2022.
[2] Climate Action Network Europe, Engaging Citizens and Local Communities in the Solar Revolution: Rooftop Solar PV Country Comparison Report, Climate Action Network Europe, 2022.
[3] C. González-Morán, P. Arboleya, V. Pilli, Photovoltaic self consumption analysis in a European low voltage feeder, Electr. Power Syst. Res. 194 (2021) 107087.
[4] S.P. Burger, J.D. Jenkins, C. Batlle, I.J. Pérez-Arriaga, Restructuring revisited part 1: Competition in electricity distribution systems, Energy J. 40 (3) (2019).
[5] A. Gómez-Expósito, A. Arcos-Vargas, J.M. Maza-Ortega, J.A. Rosendo-Macías, G. Alvarez-Cordero, S. Carillo-Aparicio, J. González-Lara, D. Morales-Wagner, T. González-García, City-friendly smart network technologies and infrastructures: The spanish experience, Proc. IEEE 106 (4) (2018) 626–660.
[6] T. Dragičević, S. Vazquez, P. Wheeler, Advanced control methods for power converters in DG systems and microgrids, IEEE Trans. Ind. Electron. 68 (7) (2020) 5847–5862.
[7] D. Kanakadhurga, N. Prabaharan, Demand side management in microgrid: A critical review of key issues and recent trends, Renew. Sustain. Energy Rev. 156 (2022) 111915.
[8] X. Xu, D. Niu, L. Peng, S. Zheng, J. Qiu, Hierarchical multi-objective optimal planning model of active distribution network considering distributed generation and demand-side response, Sustain. Energy Technol. Assess. 53 (2022) 102438.
[9] V.H. Bui, W. Su, Real-time operation of distribution network: A deep reinforcement learning-based reconfiguration approach, Sustain. Energy Technol. Assess. 50 (2022) 101841.
[10] M. Bhuyan, A.K. Barik, D.C. Das, GOA optimised frequency control of solar-thermal/sea-wave/biodiesel generator based interconnected hybrid microgrids with DC link, Int. J. Sustain. Energy 39 (7) (2020) 615–633.
[11] M. Zolfaghari, G.B. Gharehpetian, A. Anvari-Moghaddam, Quasi-luenberger observer-based robust DC link control of UIPC for flexible power exchange control in hybrid microgrids, IEEE Syst. J. 15 (2) (2020) 2845–2854.
[12] N. Okada, M. Takasaki, H. Sakai, S. Katoh, Development of a 6.6 kv - 1 MVA transformerless loop balance controller, in: 2007 IEEE Power Electronics Specialists Conference, 2007, pp. 1087–1091.
[13] W. Cao, J. Wu, N. Jenkins, C. Wang, T. Green, Operating principle of soft open points for electrical distribution network operation, Appl. Energy 164 (2016) 245–257.
[14] E. Romero-Ramos, A. Gómez-Expósito, A. Marano-Marcolini, J.M. Maza-Ortega, J.L. Martinez-Ramos, Assessing the loadability of active distribution networks in the presence of DC controllable links, IET Gener. Transm. Distrib. 5 (2011) 1105–1113(8).
[15] A. Marano-Marcolini, M. Barragan Villarejo, A. Fragkioudaki, J.M. Maza-Ortega, E. Romero Ramos, A. de la Villa Jaén, C. Carmona Delgado, DC link operation in smart distribution systems with communication interruptions, IEEE Trans. Smart Grid 7 (6) (2016) 2962–2970.
[16] D.R. Ivic, P.C. Stefanov, An extended control strategy for weakly meshed distribution networks with soft open points and distributed generation, IEEE Access 9 (2021) 137886–137901.
[17] F.P. García-López, M. Barragán-Villarejo, J.M. Maza-Ortega, Grid-friendly integration of electric vehicle fast charging station based on multiterminal DC link, Int. J. Electr. Power Energy Syst. 114 (2020) 105341.
[18] A. Hauswirth, A. Zanardi, S. Bolognani, F. Dörfler, G. Hug, Online optimization in closed loop on the power flow manifold, in: 2017 IEEE Manchester PowerTech, 2017, pp. 1–6.
[19] J.C. Olives-Camps, Á. Rodríguez del Nozal, J.M. Mauricio, J.M. Maza-Ortega, A model-less control algorithm of DC microgrids based on feedback optimization, Int. J. Electr. Power Energy Syst. 141 (2022) 108087.
[20] E.A. Rodríguez-Gonzalez, J.C. Olives-Camps, F.P. García-Lopez, A. Rodríguez del Nozal, J.M. Mauricio, J.M. Maza-Ortega, Experimental validation of a real-time distributed model-less control for DC microgrids, in: 2022 International Conference on Smart Energy Systems and Technologies, SEST, IEEE, 2022, pp. 1–6.
[21] J.C. Olives-Camps, Á.R. del Nozal, J.M. Mauricio, J.M. Maza-Ortega, A holistic model-less approach for the optimal real-time control of power electronics-dominated AC microgrids, Appl. Energy 335 (2023) 120761.
[22] L. Ortmann, A. Hauswirth, I. Caduff, F. Dörfler, S. Bolognani, Experimental validation of feedback optimization in power distribution grids, Electr. Power Syst. Res. 189 (2020) 106782.
[23] M. Picallo, S. Bolognani, F. Dörfler, Closing the loop: Dynamic state estimation and feedback optimization of power grids, Electr. Power Syst. Res. 189 (2020) 106753.
[24] K. Strunz, et al., Benchmark systems for network integration of renewable and distributed energy resources, in: CIGRE Task Force C6.04.02, 2014, p. 119.
[25] M. Picallo, L. Ortmann, S. Bolognani, F. Dörfler, Adaptive real-time grid operation via online feedback optimization with sensitivity estimation, Electr. Power Syst. Res. 212 (2022) 108405.

[26] J.M. Mauricio, J.C. Olives-Camps, J.M. Maza-Ortega, A. Gómez-Expósito, Integrated simulation of electromechanical and thermal dynamics of voltage source converters, Int. J. Electr. Power Energy Syst. 155 (2024) 109672.

[27] F.P. García-López, M. Barragán-Villarejo, A. Marano-Marcolini, J.M. Maza-Ortega, Performance assessment of flexible links in distribution networks using a detailed power losses model, IEEE Open Access J. Power Energy (2023).